CELESTE Observations of the Crab Nebula and Mkn 421 in 1999-2000 and 2000-2001

F. Piron[1], A. Jacholkowska[1] and E. Nuss[1], for the CELESTE collaboration
(1) GAM, Univ. Montpellier II, Pl. E. Bataillon, F-34095 Montpellier Cedex 5

Abstract

We report on spectral measurements starting from 50 GeV for the Crab nebula and from 70 GeV for the blazar Markarian 421. Both sources were detected by the CELESTE experiment in 1999-2000 and 2000-2001. Here we present the light curves and spectral measurements. The spectra are compared with those obtained quasi-simultaneously above 300 GeV by the CAT imaging telescope.

1. Introduction

The energy window around 50 GeV was opened by the CELESTE experiment during the winter 1999-2000 with the detection of the Crab nebula and its flux measurement above 60 GeV [1]. Nearly at the same time, CELESTE detected the blazar Markarian 421 (Mkn 421) during a series of flares. It is the first sub-100 GeV atmospheric Cherenkov detection of Mkn 421, and the emission observed by CELESTE is well correlated with the flux above 300 GeV recorded by the CAT telescope, operating on the same site [2]. The present work is an update of the first spectral analysis of these sources with CELESTE, which was reported later in [7]. The experimental setup, the γ-ray signal extraction, the energy measurement and the spectral reconstruction are briefly recalled in Sect. (2.) and Sect. (3.). In Sect. (4.) we present the results and compare them to those obtained by the EGRET and CAT detectors.

2. Experimental setup and gamma-ray signal extraction

The experimental setup of CELESTE ("CErenkov Low Energy Sampling and Timing Experiment") is fully described in [5,1]. Briefly, this detector records the Cherenkov light emitted by the secondary particles produced during the development of cosmic-ray atmospheric showers, and was designed to minimize the night-sky noise with a view to achieving a low energy threshold. Until October 2001 it used 40 heliostats ($54\,\mathrm{m}^2$ each) of the former solar plant in Thémis (French Pyrénées, altitude 1650m) and fast electronics (~1 GHz flash ADCs) suited to the duration of the Cherenkov signal (a few ns). As explained in [1], good discrimination between γ and charged cosmic-ray induced showers is achieved using the

pp. 2607–2610

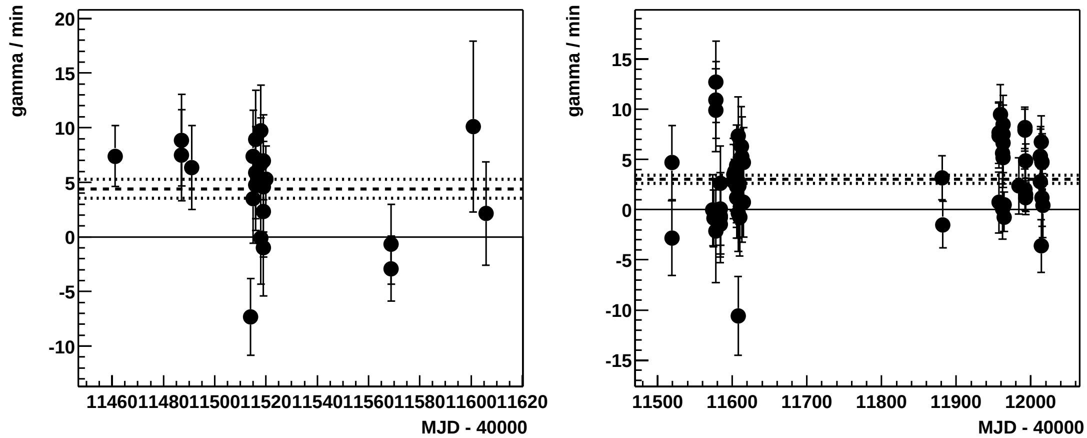

Fig. 1. The Crab nebula (left) and Mkn 421 (right) light curves between 1999 and 2001. Horizontal dashed lines show the mean flux in γ/min and its 1-σ error.

differences between both types of showers regarding the homogeneity and the time distribution of the Cherenkov light pool as sampled by the heliostats. The corresponding event selection is based on the two variables $\sigma_{\rm grp}$, which is the relative RMS of collected charge over the five heliostat groups entering the trigger logic, and θ, the shower axis angle relative to the source direction. A padding procedure and a software trigger are applied to the data to stabilize the background level near the detection threshold and to compensate for changes in the detector response (including the atmosphere) between different observations. The γ-ray signal accrues as the difference in the rate of ON and OFF-source selected events ($\sigma_{\rm grp} < 0.3$ and $\theta^2 < 50\,{\rm mrad}^2$).

3. Energy measurement and spectral reconstruction

The energy measurement method relies on the mean charge collected for all heliostats and on the shower impact parameter measured using wavefront arrival times. By restricting to intermediate values of the impact parameter, $20\ {\rm m} < P_{\rm m} < 80\ {\rm m}$, the energy can be related to the two previous variables in a very simple manner: as shown in [7], the corresponding energy resolution functions are unbiased above the detection threshold and can be well fitted by centered gaussians with resolutions varying between 12% and 24%. As explained in [7], the spectral reconstruction method starts with large energy bins with respect to the energy resolution in order to decouple energy resolution effects and acceptance corrections. Then, the *mean true energy* in each bin is estimated by a maximum likelihood fit based on an event-by-event calculation. Finally, the differential flux is obtained using a weighted acceptance over each bin. Since the latter depends on the shape of the source spectrum, which is here assumed to follow a power-law,

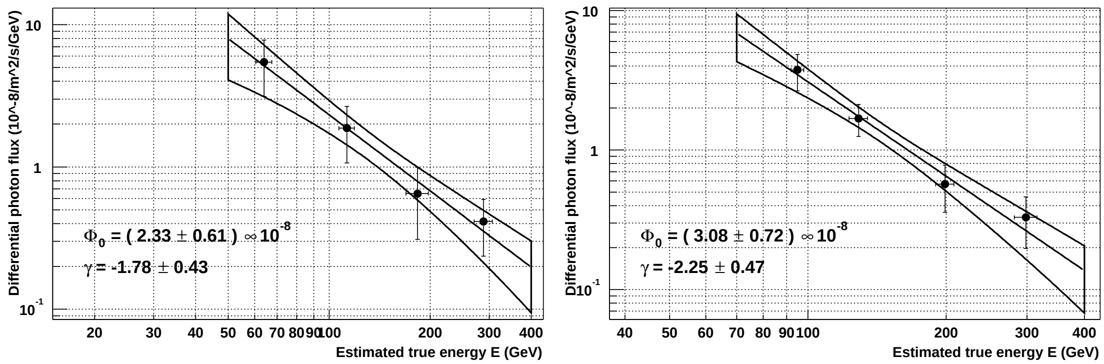

Fig. 2. Differential spectrum of the Crab nebula (left) and Mkn 421 (right), for an assumed power-law shape $\mathrm{d}N/\mathrm{d}E = \phi_0[E/100\,\mathrm{GeV}]^\gamma$. The flux constant ϕ_0 is given in units of $\mathrm{m}^{-2}\,\mathrm{s}^{-1}\,\mathrm{GeV}^{-1}$, and the outer box shows the 68% confidence level contour, taking account of the correlation between ϕ_0 and γ.

the spectral index γ is determined through an iterative procedure.

4. Results

4.1. Data samples

Data selection has been improved since [7]: it requires good weather conditions and stable detector operation, on the basis of currents and trigger rate variations during acquisition. We still restrict the analysis to the data taken near transit in order to avoid large acceptance variations. This leaves $T_{\mathrm{obs}} = 6.6$ h of ON-source data for the Crab nebula within 1h from transit (in single pointing mode), and $T_{\mathrm{obs}} = 18.1$ h for Mkn 421 mostly within 1-2h from transit (in single and double pointing mode, see [1] for details). The corresponding light curves are shown in Fig. (1.): within the selection cuts quoted in Sect. (2.), we observe a mean flux of 4.40 ± 0.86 γ/min for the Crab nebula and 3.01 ± 0.41 γ/min for Mkn 421.

4.2. Spectra

As in [7], the energy threshold for spectral reconstruction is 50 GeV for the Crab nebula and 70 GeV for Mkn 421. Here the spectra were obtained with 4 energy bins, as shown in Fig. (2.). The systematic errors we considered arise from the method recalled in Sect. (3.) and from the absolute energy scale uncertainty, which is largely dominant: assuming, like in [1,7], an uncertainty of 30%, one gets $\Delta\phi_0/\phi_0 \simeq \pm 20\%$ and $\Delta\gamma \simeq -0.30$. The broad-band SEDs are shown in Fig. (3.), which includes a proper combination of statistical and systematic errors. Note that an important difference with our preliminary results in [7] is observed in the case of the Crab nebula: mishandling of the data file for a single pair caused

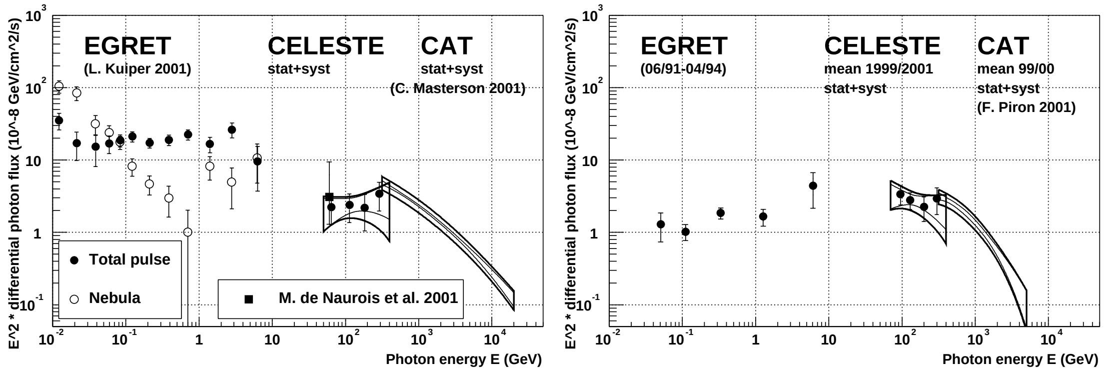

Fig. 3. The Crab nebula (left) and Mkn 421 (right) broad-band SEDs as measured by CGRO/EGRET, CELESTE ([2] and this work) and CAT. For ground-based experiments, the inner thin contours stand for statistical errors only, while the outer thick contours combine statistical and systematic errors.

an overestimate of the total signal of ∼50%. However, all these results are still compatible with the contemporary measurements above 300 GeV from the CAT telescope and, for the Crab nebula, with the flux published by CELESTE in [1]. They confirm that CELESTE is well suited to study the γ-ray peak of both sources.

5. Conclusions

The spectra of the Crab nebula and of Mkn 421 have been measured with 40 heliostats above an energy threshold of 50 GeV and 70 GeV, respectively. These spectra are compatible with contemporary results from the CAT telescope above 300 GeV. Future work will consist in the extension of the data set to larger hour angles and in the reduction of systematic errors.

6. References

1. de Naurois M. et al. 2002, ApJ 566, 343
2. Holder J. 2001, in “High-Energy Gamma-Ray Astronomy” (Heidelberg), AIP Conf. Proc. 558, ed. F. A. Aharonian & H. J. Voelk, 635
3. Kuiper L. et al. 2001, A&A 378, 918
4. Masterson C. 2001, AIP Conf. Proc. 558, 753
5. Paré E. et al. 2002, NIM A490, 71
6. Piron F. et al. 2001, A&A 374, 895
7. Piron F. et al. 2002, in “The Universe Viewed in Gamma Rays”, 25-28/09/2002 (Kashiwa, Japan), `http://icrhp9.icrr.u-tokyo.ac.jp/Symp2001.html`